TRIBOLOGY TRANSACTIONS

ISSN: 1040-2004 (Print) 1547-397X (Online) Journal homepage: http://www.tandfonline.com/loi/utrb20

The Development of a Spacer Layer Imaging Method (SLIM) for Mapping Elastohydrodynamic Contacts

P. M. Cann , H. A. Spikes & J. Hutchinson

To cite this article: P. M. Cann , H. A. Spikes & J. Hutchinson (1996) The Development of a Spacer Layer Imaging Method (SLIM) for Mapping Elastohydrodynamic Contacts, TRIBOLOGY TRANSACTIONS, 39:4, 915-921, DOI: 10.1080/10402009608983612

To link to this article: https://doi.org/10.1080/10402009608983612

VOLUME 39(1996), 4, 915–921
TRIBOLOGY TRANSACTIONS

The Development of a Spacer Layer Imaging Method (SLIM) for Mapping Elastohydrodynamic Contacts©

P. M. CANN (Member, STLE) and H. A. SPIKES (Member, STLE)
Imperial College
Tribology Section
Department of Mechanical Engineering
London, England SW72BX
and
J. HUTCHINSON
PCS Instruments
London, England SW72BH

Optical interferometry has proved to be a valuable experimental tool in the study of elastohydrodynamic lubrication (EHD). It is a technique that gives detailed information on the lubricant film distribution within the contact; however, the sensitivity is limited and it is only recently, with the development of the spacer layer optical technique, that the study of the thin film lubrication regime has been possible. The limitation of the spacer layer technique is that generally only one measurement is taken from the center of the contact. The next logical step in the development of this technique is, therefore, a system that combines the mapping capabilities of the original optical method with the thin film capabilities of the spacer layer approach.

This paper describes the development of a contact mapping technique that uses the spacer layer approach to visualize, and measure, thin lubricant films in concentrated contacts. The development of the technique is described and its application to both static and moving contacts reported. Thin EHD films (down to 10 nm) have been measured and mapped.

KEY WORDS

Elastohydrodynamic Lubrication, Optical Interferometry, Surface Films/Coatings

INTRODUCTION

The understanding of elastohydrodynamic lubrication (EHD) was advanced, in the late 1960s, by the application of optical interferometry (*1*)–(*4*) to the study of concentrated contacts. This technique gave, for the first time, a detailed map of the lubricant film thickness variation within the contact. It was pioneered by Gohar and Cameron (*1*), (*2*), who successfully mapped "classical" EHD films for different lubricants and contact conditions, thus confirming many of the predictions from analogous theoretical studies (*5*), (*6*).

Presented as a Society of Tribologists and Lubrication Engineers paper at the STLE/ASME Tribology Conference in Kissimmee, Florida, October 8–11, 1995
Final manuscript approved May 5, 1996

Therefore, the understanding of EHD, based on these theoretical and experimental studies, is such that it is now possible to predict film thickness for the classical (fully flooded, Newtonian rheology, smooth surface) regime. Many lubrication conditions, however, do not fulfill these criteria. Such systems might be considered as "non-classical" EHD and are perhaps of more practical importance. Optical interferometry has also been applied to such problems, for instance, in the study of starved (*4*) or grease-lubricated contacts (*7*) and of rough surfaces (*8*). It was in this work, however, that the limitations of the technique became apparent as in many cases the full EHD film is not formed and the film thickness drops below the normal detection limit of 80–130 nm. Study of the ensuing thin EHD or mixed regime was therefore impossible.

In recent years these limitations have been effectively overcome by the development of "thin film" optical interferometry. In this technique a silica "spacer" layer, which artificially augments the oil film, is used and thus facilitates measurement. This approach was first investigated by Westlake (*9*), who reported that films of 20 nm could be measured with a resolution of 2.5 nm in 1970. It is only recently, though, with the arrival of fast image capture and analysis methods, that it has been possible to advance this technique further (*10*). The new technique gives a single measurement from the center of the contact with an improved film thickness resolution (1 nm) and lower detection limit (2 nm). It has been successfully applied to the measurement of EHD and boundary films in the thin film and non-classical regimes. This includes low viscosity fluids (*11*), two-phase lubricants (*12*), (*13*) and in tests where the contact conditions (high temperature, starved oil supply) result in very thin EHD films (*14*), (*15*). One limitation of this technique is that it generally gives only a single measurement from the center of the contact although some work on contact profiling has been reported (*16*). In classical "thick" film EHD (>130 nm), the film shape is well understood and this measurement is sufficient to define the characteristics of the contact. In the thin film and non-classical regimes, little is known of the film shape and the way in which this is determined by the lubri-

cant, surface properties or contact conditions. Lubrication models do exist for the thin film regime (*17*) but, as yet, they have not been verified by experimental results.

The next step, therefore, is the development of a technique, to give contact maps, that combines the sensitivity of the thin film technique with the mapping capabilities of the normal optical method. It is the development and application of such a technique that is described in this paper. The spacer layer imaging method (SLIM) is based on the existing thin film optical technique (*10*). The aim was to develop a technique capable of providing film thickness maps from an EHD contact operating in the thin film regime (10–80 nm). The use of color image analysis to give such maps is not new, but such work has been confined to the classical EHD regime (>100 nm) (*18*). The new technique will be used, therefore, to explore film shape, and the influence of fluid and surface properties, in the thin film regime from 10–150 nm.

DEVELOPMENT OF TECHNIQUE

In optical interferometry, the EHD contact is usually formed by a glass or sapphire disc loaded and moving against a steel ball, as shown in Fig. 1. The motion can either be rolling or sliding or a mixture of both. The contact is viewed through a microscope positioned immediately above the contact. The underside of the glass disc is coated with a semi-reflecting chromium layer to give the necessary reflection conditions for the interference fringes. Visible light (white light or monochromatic) is shone vertically into the contact and reflection occurs at both the chromium/oil and oil/steel interfaces. The reflected beams are then recombined to give an interference pattern. A series of interference fringes is thus seen by the observer where the color and fringe order correspond to the different film thicknesses. In the original optical technique, a 2-D image is obtained where the film thickness variation is seen as color contours within the contact. The measurement range is typically 80 nm to 1 μm. The minimum film thickness detectable is related to the interference wavelength and is usually 80–130 nm. For polychromatic interferometry, the value of 130 nm is usually taken as the lower limit with a thickness resolution of 25–30 nm.

In the thin film technique shown in Fig. 1 (*10*), the chromium layer is overlaid by a silica film that augments the oil film and, thus, effectively removes the 100 nm limitation. The image from the contact is dispersed through a spectrometer and captured by a CCD camera. The image from the camera is analyzed to give an intensity versus wavelength distribution so that the wavelength of maximum constructive interference can be determined with nanometer accuracy. It is necessary to take a zero reading of the silica film thickness at the start of the test; the ball is loaded against the glass disc and a static measurement taken. This value is then subtracted from subsequent lubricant film measurements. It is this combination of spacer layer and image analysis techniques that gives the improvement in both the minimum detectable thickness (1 nm) and thickness resolution (1 nm).

The thin film optical technique is used as the basis for the development of the current method, as the spacer layer can be used in a similar way to help "visualize" the EHD film

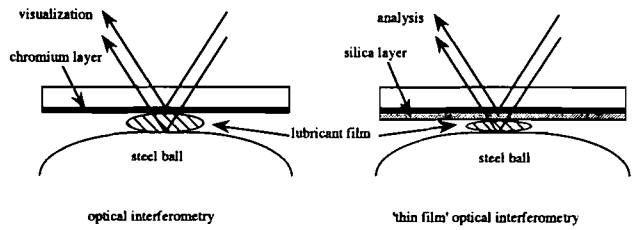

Fig. 1—Optical interferometric measurement of EHD films.

over the entire contact. The presence of the silica layer augments any thin lubricant film, making it visible as a second or third order interference color. A color CCD camera is used to capture an image of the contact which is then translated into a color bit map. This can then be converted into an absolute film thickness map by using a suitable color/film thickness calibration and subtracting the original zero silica thickness measured at the start of the test.

Description of System

The basic system is shown in Fig. 2. It comprises a color CCD camera mounted on the draw tube of a microscope. The image is focused through an objective using a collimated, high intensity light source. The image is illuminated through the objective using a beam splitter arrangement mounted between the objective and camera. The image can be recorded on a standard video recorder or captured and stored for subsequent analysis. The camera used was a JVC (TK-107E) with a variable shutter speed down to 0.00001 second. This fast shutter speed is necessary if clear images of local features within a moving contact are to be obtained. However, the fast shutter speed requires an intense light source and good light gathering optics. In the current system, a tungsten halogen source with fiber optic light guide is used to illuminate the contact. A Zeiss ×5 objective is used to image the contact. This objective combines efficient light gathering with a long working distance and is corrected for chromatic aberration.

The camera output is S-VHS which contains two signals: chrominance and luminance. The frame grabber converts these internally into separate red, green and blue signals that are digitized and stored. The software then converts the stored color values into hue, saturation and intensity. At present, it is the hue value that is used to define the image color and is calibrated against film thickness. The hue reading has

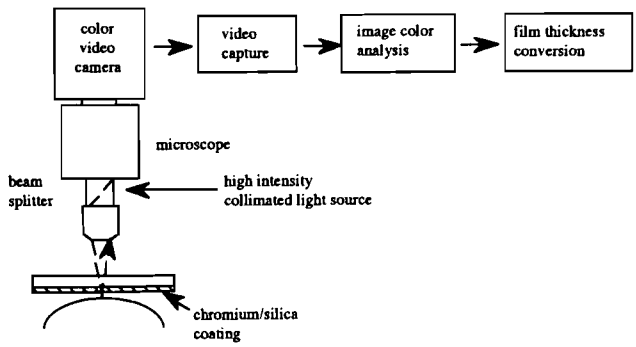

Fig. 2—Spacer layer imaging system.

values from 0 to 360 within which "pure red" can be arbitrarily assigned to zero, "pure blue" to 240 and "pure green" to 120.

The image capture is triggered by setting a shaft encoder position. Subsequent images are then taken from the same position on the disc. This is important if the relevant zero spacer layer thickness is to be used.

Calibration

One of the first requirements was to obtain a hue/wavelength or hue/film thickness calibration. The existing thin film technique was used to calibrate hue in terms of both wavelength and film thickness. The following method was used:

1. A glass disc with the underside coated with both chromium and silica layers is loaded against a steel ball forming a stationary Hertzian contact.
2. The conventional thin film technique is used to measure the interference wavelength. The image from the contact is focused onto a spectrometer which gives an intensity/wavelength profile which is captured by CCD camera. The wavelength of constructive interference can now be determined accurately through image analysis. This gives a measurement of the local silica layer thickness.
3. The thin film optics are then replaced by the imaging camera and the corresponding hue value measured. The thin film technique measures an average thickness across the contact. To obtain a representative hue value, it was necessary to sample from several areas within the contact and calculate an average.

The hue against wavelength data is transformed into hue against silica film thickness (for different orders) by applying a suitable phase change correction and dividing by the silica refractive index:

$$h_{\text{film thickness}} = [h_\lambda(N - \phi)]/2n$$

where h_λ = wavelength of constructive interference, N = order, n = refractive index of layer and ϕ = phase change.

The resulting hue versus silica film thickness plot is shown in Fig. 3 for Orders 2 and 3. The magnification and image capture size used in this work gives a spatial resolution of 3 μm (per pixel). The estimated film thickness resolution is 5 nm.

The hue/silica thickness results have been curve-fitted and a suitable calibration developed. This calibration is used to determine the "zero" silica film thickness at the start of the test and the additional EHD film developed during the test. At present, a single refractive index (1.45) is used for both the silica layer and oil film. In future work, a refractive index correction for the oil film will be used.

The following procedure is used to obtain a film thickness profile:

1. A glass disc with a suitable chromium/silica layer coating is loaded against the steel ball and the CCD camera focused into the contact.

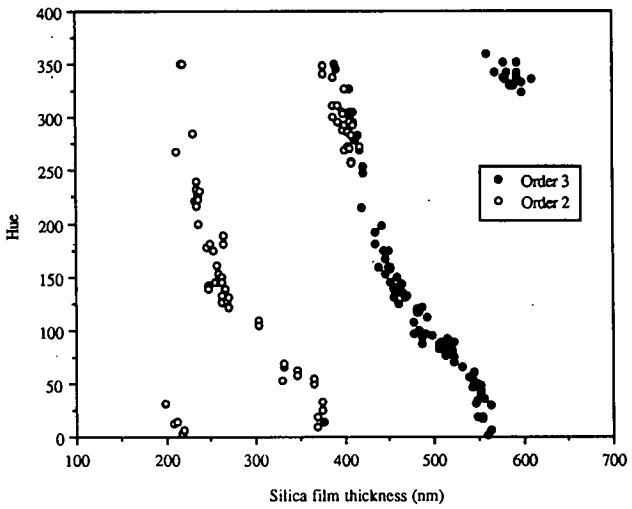

Fig. 3—Hue as a function of silica film thickness.

2. The encoder trigger position is selected and a zero silica layer reading taken.
3. Lubricant is applied to the disc and the test started. To capture an image the system is set to trigger at the defined encoder position.
4. Captured images are stored for subsequent analysis.

The captured images are first converted into a hue map and from this to combined (silica layer + oil) film thickness. To do this, an interference order must be defined for one point in the contact and the calibration is then used to calculate film thickness from this starting position for the entire contact. The zero silica layer thickness is then subtracted from the combined measurement. The contact geometry can then be plotted as a 3-D map or as simple 2-D film thickness profiles taken at different positions within the contact. In this paper, the results are confined to profiles taken either transverse or parallel to the direction of rolling along the contact center line. Examples of captured images and the resulting film thickness profiles are shown later in this paper.

RESULTS AND DISCUSSION

Examples of images from both stationary and moving contacts are presented. The results of the subsequent film thickness analysis are compared with theoretical predictions wherever possible.

Stationary Contact Profiling

A captured image from a stationary contact, for a load of 36N, is shown in Fig. 4. The presence of the spacer layer gives the blue color in the central Hertzian region. It is possible to take a profile across the contact and this is shown in Fig. 5 as a *displacement* profile (measured distance from the chromium reference layer). The zero silica layer thickness has already been subtracted from these results. The profile is compared to the calculated Hertzian deformation profile (shown as a plain line) and good agreement is seen between the experimental and theoretical result. The surface finish of the ball was measured as 0.012 μm Ra. It is to be expected that surface asperities will elastically conform to one another

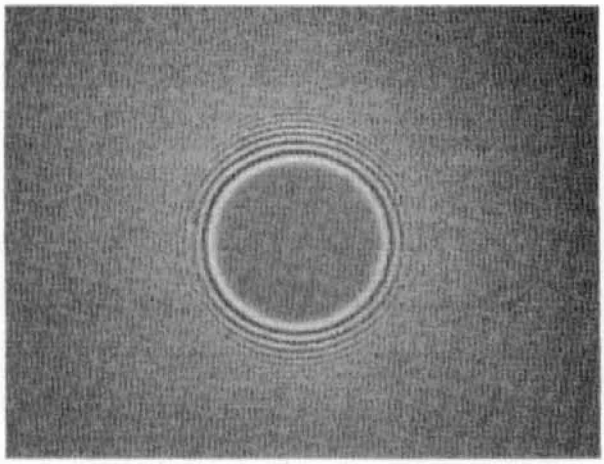

Fig. 4—Captured image from a stationary Hertzian contact with a silica layer.

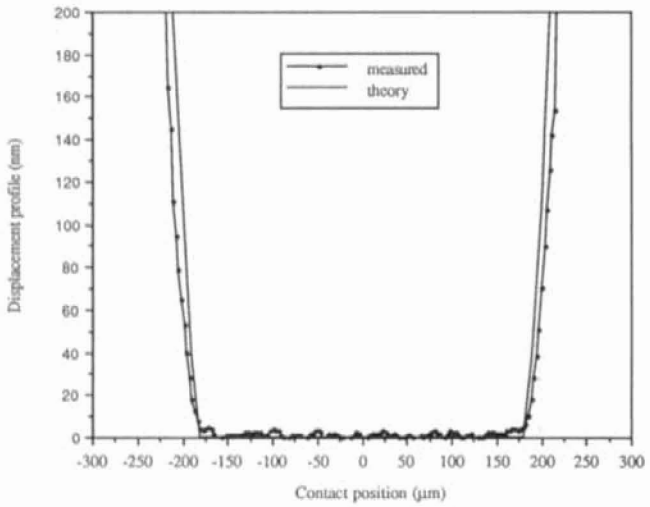

Fig. 5—Displacement profile across Hertzian contact from Fig. 4.

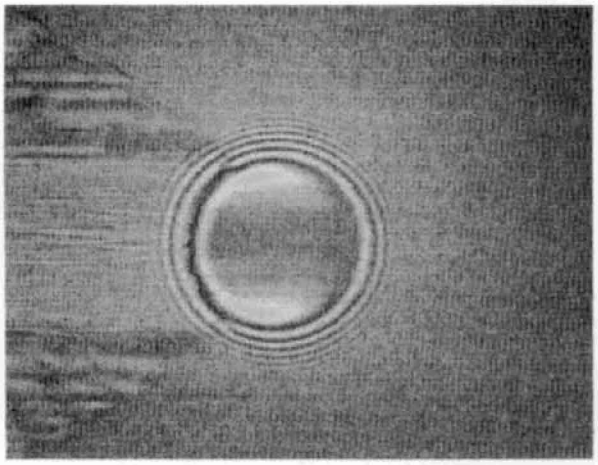

Fig. 6—Captured images from a starved fluid film-lubricated contact.

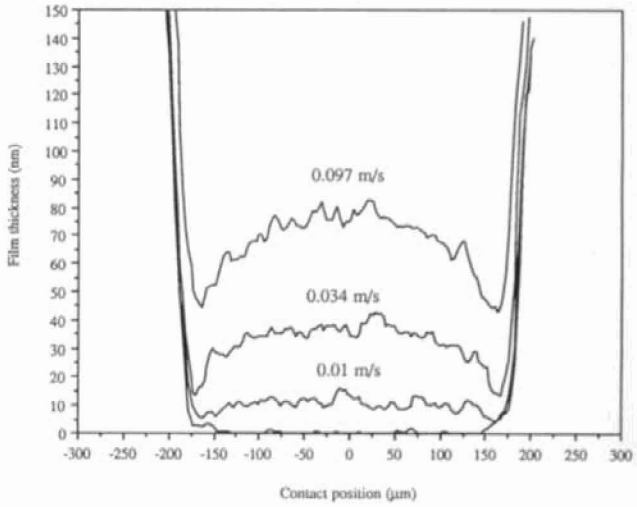

Fig. 7—Film thickness profiles (transverse to rolling direction) of a fluid film EHD contact.

in the Hertzian region although minor surface irregularities (1–2 nm) can be seen in the profile.

EHD Lubricant Film Profiling

Classical EHD

An image of a classical EHD film is shown in Fig. 6. The film shown is a synthetic poly-α-olefin (SHC) oil (viscosity 0.056 PaS at 20°C, load 17N) at 0.2 m/s. EHD film thickness was also calculated for this condition using the classical Dowson and Hamrock equations (*19*). Thus, the calculated central film thickness (h_c) for this condition was 133 nm and the minimum (h_m) 68 nm (*19*). This compares to measured values of 129 and 60 nm, respectively.

Figure 7 film shows thickness profiles, taken across the center line transverse to the rolling direction, for a series of images taken at different speeds. The development of the characteristic EHD film shape can clearly be seen. At the lowest speed (0.01 ms^{-1}), the side lobes are just visible; they become more pronounced as the speed increases. The film profiles obtained are not smooth, showing significant thickness fluctuations. This is attributed to the surface roughness variation on the steel ball, rather than the glass disc, as the latter is much smoother and is not thought to contribute significantly to the combined surface roughness. Talysurf measurement of the (undeformed) ball surface gave an Ra of 0.012 μm. In the static contact these asperities elastically conform, giving only minor fluctuations of less than 3 nm. With increasing film thickness, the fluctuations increase from an average of 6 nm at 0.034 ms^{-1} to 9 nm at 0.097 ms^{-1}. This is to be expected if the overall elasticity of the film increases as its thickness increases.

The film thicknesses measured by SLIM have been compared to calculated values (*19*). The SLIM values were obtained by drawing a smooth curve through the profile, thus averaging the fluctuations in the central region. These film thickness results, both h_c and h_m, are compared to calculated (smooth surface) values (shown as solid lines) in Fig. 8 (*19*). Good agreement is seen for the central film thickness down to below 30 nm. The results for the minimum film thickness are generally lower than predicted although they do converge as the film increases. It is probable that the local surface roughness reduces the film thickness compared to the smooth surface predictions (*8*).

Starved Lubricant Film Formation

One of the possible applications of this technique is in

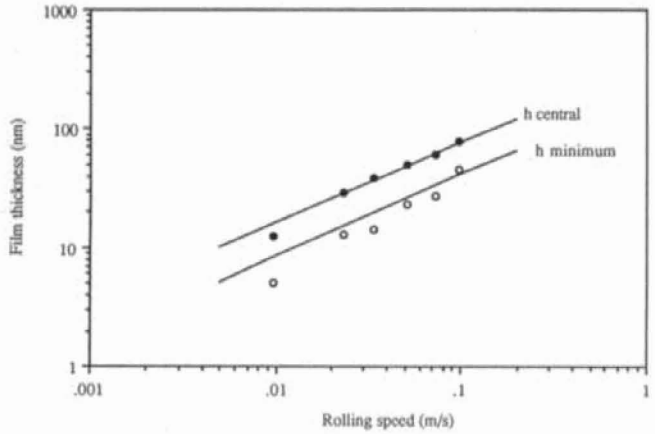

Fig. 8—Comparison of measured and calculated film thickness results for SHC fluid (20°C, 36N).

profiling thin EHD films formed under "non-classical" conditions, e.g., in a starved lubricated contact. Starvation occurs when there is insufficient lubricant to fill the inlet of the conjunction and an air/oil meniscus occurs close to the contact. As a result, the lubricant does not experience the full pressure buildup and a reduced EHD film is formed. The onset of starvation is controlled by the amount of oil flowing back into the track and, hence, the amount and viscosity of the fluid and the rotation speed (time between overrollings). A typical starvation curve is shown in Fig. 9 where film thickness is plotted with increasing speed. A restricted amount of oil is initially applied to the disc in this test and the film thickness is measured with increasing speed. These results are from the thin film optical technique where a single (averaged) measurement is taken from the central region. At slow speeds, the film increase is as expected for a fully flooded contact. However, at a certain critical speed, the film thickness deviates from the fully flooded curve and then drops with further increases in speed. The EHD regime in this test moves from the fully flooded (a) to the starved (b) and then parched (c) condition where there is a little reflow into the track and an almost speed independent film is observed (*14*).

In Fig. 10, a series of captured images from a starved EHD contact is shown (rolling direction is from right to left). In this test, starvation was induced by progressively removing oil from the rolling track while keeping the speed constant ($0.155\ ms^{-1}$). A direct comparison of the fully flooded and starved film profiles can then be made. The corresponding film thickness profiles (taken transverse to the rolling direc-

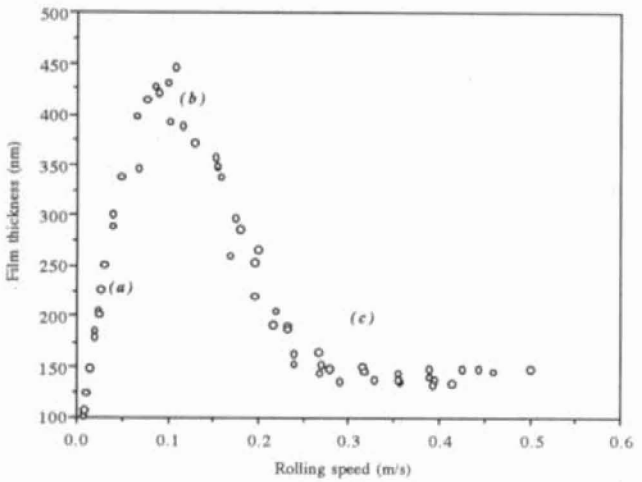

Fig. 9—Central film thickness *vs.* rolling speed starvation curve.

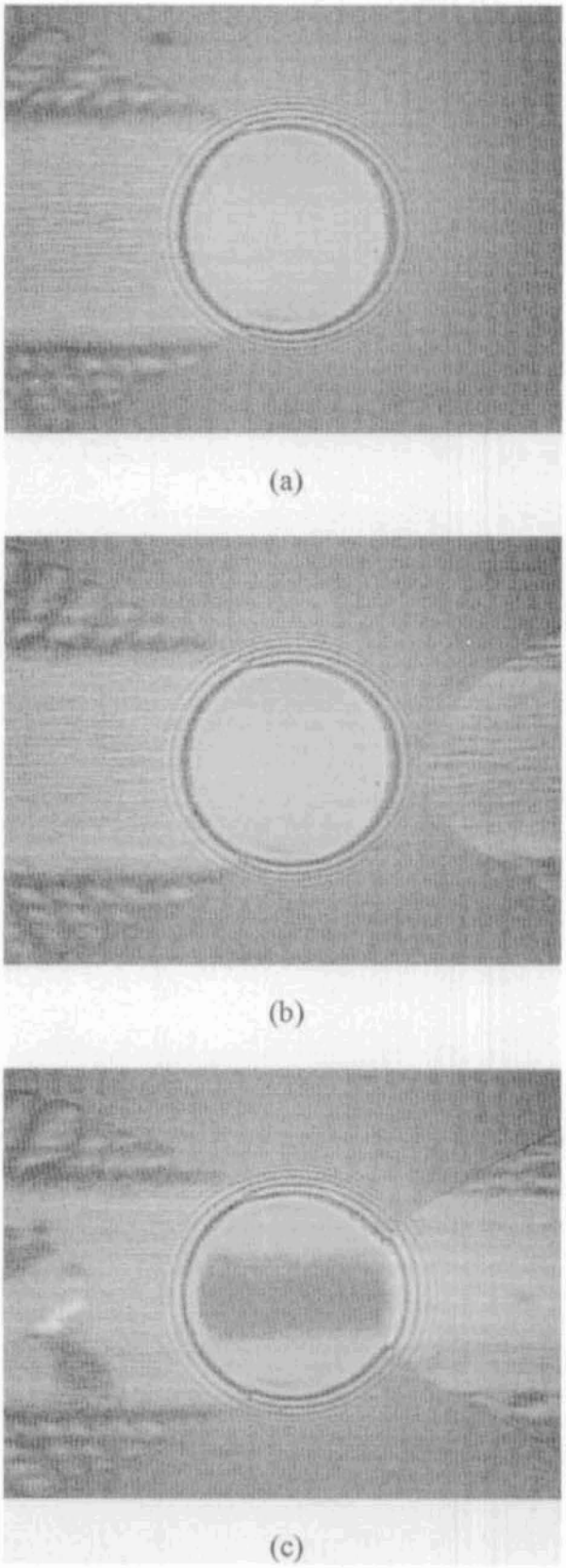

Fig. 10—Captured images from a starved lubricated contact.

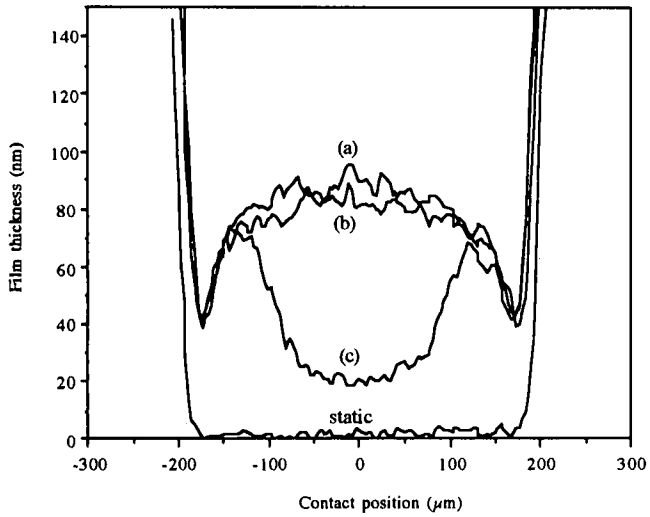

Fig. 11—Comparison of "fully" flooded and starved film thickness profiles (transverse to rolling direction) for SHC oil (0.155 ms^{-1}, 20°C).

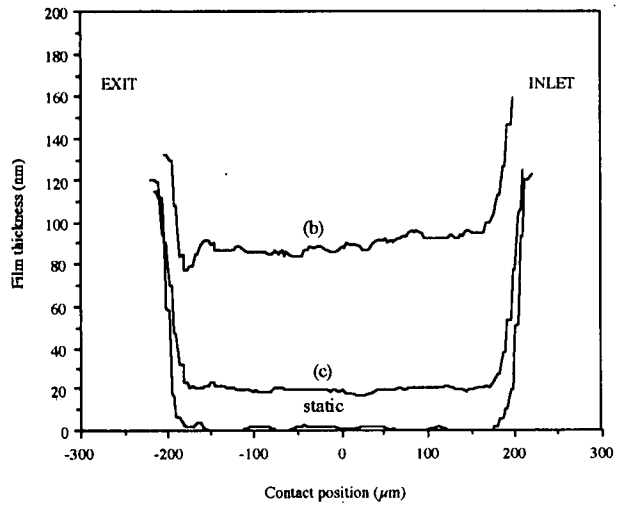

Fig. 12—Comparison of "fully" flooded and starved film thicknes profiles (through center line parallel to rolling direction) for SHC oil (0.155 ms^{-1}, 20°C).

tion) are shown in Fig. 11. In Fig. 10(a) the inlet is fully flooded and a central film of 90 nm (shown in Fig. 11, Plot (a)) was measured; this compares to a calculated value of 93 nm. The measured film thickness in the side lobes was 40 nm (calculated 50 nm). With increasing oil removal the oil/air meniscus approaches the contact, as shown in Fig. 10(b) and a decrease in central film thickness occurs to 85 nm (average), as shown in Fig. 11, Plot (b). This is the starved condition corresponding to (b) above. With yet further starvation, the oil meniscus is no longer visible outside the contact and the central film thickness drops to 20 nm with a side lobe thickness of 35 nm. This is the heavily starved or parched regime of (c). It is interesting that for the heavily starved contacts the minimum film thickness is now in the center of the contact rather than at the side lobes. Film profiles taken parallel to the rolling direction are shown in Fig. 12 and correspond to the images: static, (b) and (c) from Fig. 10. These profiles taken along the center line of the contact show that as starvation increases, fluid pressure buildup no longer occurs in the central region and the film shape approaches Hertzian (Fig. 12). It is expected that the pressure profiles for this condition are greatly distorted and do not show the classical EHD film distribution. Although these effects have been observed and qualitatively described before, it has not been previously possible to obtain film thickness profiles for the extreme starved condition.

The starved film profiles shown are in general agreement with earlier observations (*4*), (*20*). Wedeven (*4*) also noted that the distribution of the oil in the inlet region determined the film thickness attained in the contact. Theoretical studies of starved elliptical contacts have used a defined inlet boundary distance to determine the onset of starvation and, hence, calculate the film profile (*21*). However, this approach does not include a realistic inlet boundary shape and, hence, oil distribution, nor can it be used to model the heavily starved regime shown in Fig. 11, Plot (c). The importance of the inlet film distribution and its contribution to the observed film shape has also been demonstrated in numerical studies of hydrodynamically lubricated contacts (*22*).

At present, the film thickness resolution of this technique is considered to be 10 nm. Therefore, it is not as accurate as the single measurement thin film technique (1 nm). The main source of error is the calibration curve, for the hue against film thickness, as this is not linear over the measurement range. The results have been curve fitted and a calibration curve developed; however, this needs further work to verify that the entire range is accurate. At the low wavelength side the gradient is steep and there is little change in film thickness with hue, so the results are relatively insensitive to calibration error. As the wavelength increases the film thickness dependence on the change in hue increases. Therefore, it is expected that measurements taken at lower hue values will be more sensitive to calibration error.

The technique does not use intensity changes as a basis for measurement as they are inherently more sensitive to error from operating variables, e.g., changes in surface reflectivity, light source output, camera response and mechanical vibration. The advantage of this technique is that the measured hue is relatively insensitive to variations in camera and light source operation.

CONCLUSIONS

The conclusions from this work can be summarized as follows:

1. An imaging system has teen developed to give accurate film thickness profiles of EHD contacts in real time.
2. The thickness range is 0–150 nm with an estimated resolution of 5 nm. The spatial resolution is currently 3 μm.
3. Film thickness profiles have been taken for both static and moving contacts. The film thickness results have been compared to theoretical predictions where possible and good agreement is found.
4. The technique can be used to give detailed information on EHD film thickness and shape for the non-classical

regime. Examples are given for a heavily starved contact. It is envisaged that future applications will include rough surface EHD, two-phase lubricants and high pressure contacts.

REFERENCES

(*1*) Gohar, R. and Cameron, A., "Theoretical and Experimental Studies of the Oil Film in Lubricated Point Contacts," *Proc. Roy. Soc.*, **A 291,** pp 520–536, (1966).

(*2*) Gohar, R. and Cameron, A., "The Mapping of Elastohydrodynamic Contacts," *ASLE Trans.*, **10,** pp 215–225, (1966).

(*3*) Foord, C. A., Hammann, W. C. and Cameron, A., "The Evaluation of Lubricants Using Optical Elastohydrodynamics," *ASLE Trans.*, **11,** pp 31–43, (1968).

(*4*) Wedeven, L. J., "Optical Measurements in Elastohydrodynamic Rolling-Contact Bearings," Ph.D. Dissertation, London University, London, (1970).

(*5*) Gentle, C. R., Duckworth, R. R. and Cameron, A., "Elastohydrodynamic Film Thickness at Extreme Pressures," *ASME Jour. Lubr. Tech.*, **97,** pp 383–389, (1975).

(*6*) Wan, G. T., "Elastohydrodynamic Film Thickness of Water-based Hydraulic Fluids," Ph.D. Dissertation, London University, London, (1983).

(*7*) Rasteger, F. and Winer, W. O., "On the Traction and Film Thickness Behaviour of Grease in Concentrated Contact," *NLGI Spokesman*, **50,** pp 162–174, (1986).

(*8*) Kaneta, M., Sakai, T. and Nishikawa, H., "Effects of Surface Roughness on Point Contact EHL," *Trib. Trans.*, **36,** pp 605–612, (1993).

(*9*) Westlake, F. J., "An Interferometric Study of Ultra Thin Films," Ph.D. Dissertation, London University, London, (1970).

(*10*) Johnston, G. J., Wayte, R. C. and Spikes, H. A., "The Measurement and Study of Very Thin Lubricant Films in Concentrated Contacts," *ASLE Trans.*, **34,** pp 187–194, (1991).

(*11*) Guangteng, G. and Spikes, H. A., "Behaviour of Lubricants in the Mixed Elastohydrodynamic Regime," in *Proc. of the 21st Leeds-Lyon Symp.*, pp 479–486, (1995).

(*12*) Barker, D., Johnston, G., Spikes, H. A. and Bunemann, T., "EHD Film Formation and Starvation of Oil-in-Water Emulsions," *Trib. Trans.*, **36,** pp 565–572, (1993).

(*13*) Cann, P. M. and Spikes, H. A., "Thin Film Optical Interferometry in the Study of Grease Lubrication in a Rolling Point Contact," *Acta Tribologica*, **2,** pp 45–50, (1994).

(*14*) Guangteng, G., Cann, P. M. and Spikes, H. A., "A Study of Parched Lubrication," *Wear*, **153,** pp 91–105, (1992).

(*15*) Gunsel, S., Aderin, M. E. and Spikes, H. A., "In-Situ Measurement of ZDDP Films in Concentrated Contacts," *Trib. Trans.*, **36,** pp 276–282, (1993).

(*16*) Aderin, M. E., "Interferometric Studies of Very Thin Lubricant Films in Concentrated Contacts," Ph.D. Dissertation, London University, London, (1994).

(*17*) Tichy, J., "Modelling of Thin Film Lubrication," *Trib. Trans.*, **38,** pp 108–118, (1995).

(*18*) Gustafsson, L., Höglund, E. and Marklund, O., "Measuring Lubricant Film Thickness with Image Analysis," *Proc. IMechE,* **208,** pp 109–205, (1994).

(*19*) Hamrock, B. J., "Fundamentals of Fluid Film Lubrication," McGraw Hill, London, p 474, (1994).

(*20*) Ranger, A. P., "Numerical Solutions to the Elastohydrodynamic Equations," Ph.D. Dissertation, London University, London, (1974).

(*21*) Hamrock, B. J. and Dowson, D., "Isothermal Elastohydrodynamic Lubrication of Point Contacts. Part IV—Starvation Results," *Jour. Lubr. Tech.*, **99,** pp 15–23, (1977).

(*22*) Chevalier, F., Lubrecht, A. A., Cann, P. M. E., Dalmaz, G. and Colin, F., "Starved Fluid Film Lubrication—A Qualitative Explanation," in *Proc. of the 21st Leeds-Lyon Symp.*, pp 249–257, (1995).